Brazilian Journal of Analytical Chemistry
Pre-publication – Accepted after peer review
doi: 10.30744/brjac.2179-3425.AR-71-2025

BrJAC

ARTICLE

Laser-Induced Graphene Sensor for Electrochemical Determination of Nimesulide

Mylla Karliane Vera Cruz Fróz[1], Dianderson Cristiano Monteiro Ferreira[2], Matheus Barros Garcez[1], Gustavo Carvalho Diniz[3], Luiz Ricardo Guterres e Silva[1], Jéssica Santos Stefano[4], Auro Atsushi Tanaka[1], Iranaldo Santos da Silva[4], Luiza Maria Ferreira Dantas*[4]

[1]Universidade Federal do Maranhão, Departamento de Química, São Luís, MA, 65080-805, Brazil
[2]Universidade Federal de Uberlândia, Instituto de Química, Uberlândia, MG, 38408-100 Brazil
[3]Instituto Federal de Educação, Ciência e Tecnologia do Maranhão, São Luís, MA, 65030-005, Brazil
[4]Universidade Federal do Maranhão, Departamento de Tecnologia Química, São Luís, MA, 65080-805, Brazil

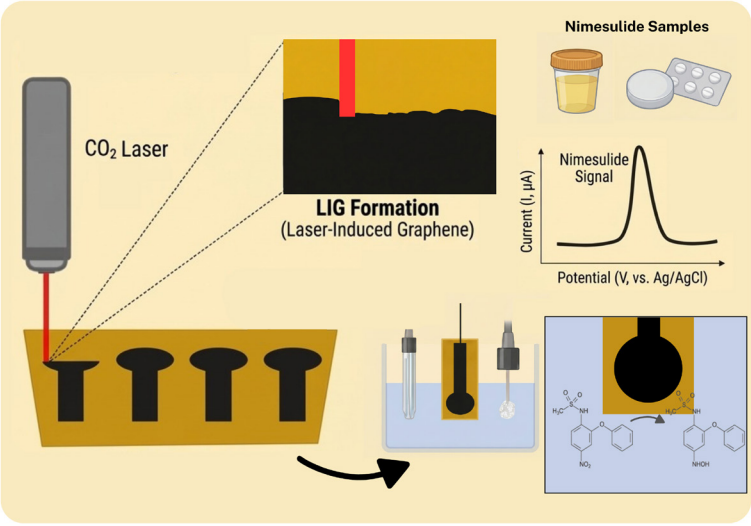

Part of this graphical abstract was generated with the assistance of the Google Gemini AI tool. The final figure was reviewed by the authors, who take full responsibility for its content.

Nimesulide (NMS) is a sulfonamide-class non-steroidal anti-inflammatory drug widely used in pharmaceutical formulations, whose reliable quantification is essential for quality control. In this work, an unmodified laser-induced graphene electrode (LIGe), fabricated by direct CO_2 laser ablation of polyimide, is proposed for the electrochemical determination of NMS using square-wave voltammetry (SWV). Voltammetric studies revealed that NMS oxidation is an irreversible, diffusion-controlled process that involves the transfer of two protons and two electrons. After systematic optimization of pH and instrumental parameters, the method exhibited a wide linear working range from 11.0 to 131 μmol L^{-1}, with a detection limit of 1.30 μmol L^{-1}. The sensor showed good repeatability (RSD < 5%, n = 10) and was successfully applied to the analysis of pharmaceutical tablets, yielding results consistent with the declared content. Accuracy was further evaluated in synthetic urine, with recovery rates between 97% and 111%. Interference studies demonstrated that common non-electroactive urinary constituents caused only minor signal variations (<3%). Although the detection limit is higher than that reported for heavily modified electrodes, the proposed approach offers simplicity of fabrication, rapid analysis, disposability,

Cite: Fróz, M. K. V. C.; Ferreira, D. C. M.; Garcez, M. B.; Diniz, G. C.; Guterres e Silva, L. R.; Stefano, J. S.; Tanaka, A. A.; da Silva, I. S.; Dantas, L. M. F. Laser-Induced Graphene Sensor for Electrochemical Determination of Nimesulide. *Braz. J. Anal. Chem.* (Forthcoming). https://doi.org/10.30744/brjac.2179-3425.AR-71-2025

Submitted: August 18, 2025; **Revised:** February 4, 2026; **Accepted:** March 10, 2026; **Published online:** April 2026.

This article was submitted to the BrJAC special issue on the 21st ENQA and 9th CIAQA.

and a broad linear range, which are notably advantageous for pharmaceutical quality control applications where analyte concentrations are relatively high. These results highlight unmodified LIG as a practical, cost-effective, and scalable sensing platform for routine nimesulide analysis.

Keywords: nimesulide, laser-induced graphene electrode, electrochemical detection, pharmaceutical analysis

INTRODUCTION

Nimesulide (NMS) is a non-steroidal anti-inflammatory drug (NSAID) belonging to the sulfonamide class, with analgesic and antipyretic properties.[1,2] It is widely prescribed in Brazil due to its superior efficacy compared to similar drugs such as diclofenac, ibuprofen, and piroxicam.[3] Despite its advantages, including low cost and rapid onset of action, indiscriminate administration, particularly at high doses or in combination with other drugs, can lead to severe side effects, including gastric, hepatic, and renal damage, as well as renal insufficiency and hepatotoxicity.[4-8] NSAIDs are one of the most widely used classes of drugs worldwide, employed in treating acute and chronic pain associated with inflammatory processes. These drugs possess anti-inflammatory, analgesic, and antipyretic properties, which stem from their ability to inhibit prostaglandin synthesis by blocking cyclooxygenase enzymes COX-1 and COX-2. This action has led to the creation of subgroups of selective and non-selective COX-2 inhibitors.[9] NSAIDs are primarily used to alleviate symptoms of osteoarthritis, rheumatoid arthritis, fever, and pain.[6]

Various analytical techniques, such as spectrophotometric and chromatographic methods with UV-vis or mass spectrometric detection[10,11] have been employed to determine NMS. However, these techniques are often associated with high costs, complex sample pre-treatment steps, and the generation of toxic waste.[12] In this regard, electroanalytical methods offer several advantages over conventional approaches, including lower reagent consumption, shorter analysis time, lower instrumentation costs, and fewer toxic reagents.[13]

In electroanalytical techniques, the choice of the working electrode is fundamental for the development of analytical methods.[13] Among carbon-based materials, graphene has emerged as a prominent option due to its high electrical conductivity, large surface area, and mechanical strength.[14] A particularly attractive form is laser-induced graphene (LIG), which is produced through a direct and rapid laser scribing process that converts sp^3 carbon into sp^2 carbon on polymeric substrates. This fabrication method is simple, cost-effective, and scalable, eliminating the need for complex synthesis steps and chemical treatments typically required for graphene production.[15,16]

Laser-induced graphene electrodes (LIGe) have shown promise in pharmaceutical detection. Recent studies have demonstrated its efficacy as a portable platform for the electrochemical detection of tyrosine[15] and ivermectin,[17] employing voltammetric techniques that exhibited broad linear ranges, low detection limits, and good selectivity against interferents. However, to our knowledge, no studies have reported the use of LIG for the analysis of NMS. In fact, only one work describes the use of LIG for the determination of NSAID. Wanjari et al. (2024)[18] report the use of two different LIGs (based on Poly(ether sulfone) – PES, and polyimide – PI substrates) for the analysis of diclofenac. The authors explored the adsorptive and spontaneous interaction of diclofenac with LIG and applied the sensors in the analysis of the NSAID in water samples.

Although laser-induced graphene (LIG) has been widely explored as a versatile platform for electrochemical sensing, most reported LIG-based sensors rely on chemical modification, nanoparticle decoration, or biofunctionalization to achieve enhanced sensitivity. Similarly, the majority of electrochemical methods reported for nimesulide determination employ multi-step electrode modification strategies, such as carbon paste formulation with modifiers, nanocomposite synthesis, or polymer electrodeposition, to reach ultralow detection limits. While these approaches are effective for trace-level analysis, they often increase fabrication complexity, preparation time, and batch-to-batch variability.

In this context, the present work addresses a practical gap by investigating the use of unmodified polyimide-based laser-induced graphene (LIG) electrodes for nimesulide determination. Rather than targeting the lowest possible detection limit, the proposed approach focuses on achieving a wide linear working range combined with minimal fabrication complexity, aiming at applications where analyte concentrations are relatively high and rapid, low-cost analysis is required. In this study, NMS was successfully determined in pharmaceutical formulations and synthetic urine using an unmodified disposable LIG electrode fabricated by CO_2 laser ablation of polyimide (Kapton). Square-wave voltammetry (SWV), fully optimized with respect to pH and instrumental parameters, provided fast voltammetric responses enabling straightforward NMS quantification without electrode modification or complex sample pretreatment. As a result, the sensor proved to be a reliable, cost-effective, and efficient tool for NMS determination in pharmaceutical and simulated biological matrices, highlighting its potential for routine quality control and preliminary clinical applications.

MATERIALS AND METHODS

Reagents and solutions

All reagents used in this work were of analytical grade and used as received. The aqueous solutions were prepared with high-purity deionized water with a resistivity of at least 18 MΩ cm, obtained from a Millipore Direct 8 water purification system (Millipore®, Germany). A stock solution containing 5.0 mmol L^{-1} NMS (Sigma-Aldrich®, USA) was prepared in 0.10 mol L^{-1} sodium hydroxide (Isofar®, Brazil). Prior to conducting the experiments, this solution was diluted using a suitable supporting electrolyte. A 0.12 mol L^{-1} Britton-Robinson (BR) buffer solution was formulated from acetic acid, boric acid, phosphoric acid, and potassium chloride reagents (Isofar®, Brazil). Additionally, a 0.10 mol L^{-1} phosphate buffer (PB) solution was prepared with monosodium phosphate and disodium phosphate (Isofar®, Brazil).

Preparation of the electrode

The LIGe was fabricated using a WorkSpecial WS4040 CO_2 laser cutter (São Paulo, Brazil) equipped with a 10.6 μm wavelength laser and a total power of 40 W. The electrode design was created using RDWorks 8.0 software and fabricated using a power of 0.9 W, a pulse duration of 14 μs, and a printing speed of 40 mm s^{-1}. The laser was positioned 10 mm above the polyimide substrate, and a batch of four electrodes was produced within 280 seconds. To delimit the working electrode area, a layer of commercial colorless nail polish was applied. After drying at room temperature, a copper tape was used to establish improved electrical contact.[17]

Electrochemical measurements

Experiments involving cyclic voltammetry (CV) and square wave voltammetry (SWV) were conducted using an Autolab PGSTAT-128N potentiostat/galvanostat (Metrohm Autolab, Utrecht, Netherlands). This equipment was connected to a microcomputer and operated with NOVA 2.2.1 software, in conjunction with a non-heating magnetic stirrer (Fisatom, São Paulo, Brazil). Baseline correction was applied to all experiments data using the moving average mode (window size 2) within the NOVA 2.2.1 software. Electrochemical tests were conducted in a cylindrical electrochemical cell with an internal volume of approximately 10 mL. A platinum wire served as the counter electrode, a miniaturized Ag|AgCl|KCl (3.0 mol L^{-1}) reference electrode was used, LIGe functioned as the working electrode, and magnetic stirring was employed between measurements.

Sample preparation

Pharmaceutical samples containing 100 mg of NMS per tablet were purchased from local drug stores in São Luís, MA, Brazil. Ten tablets were finely ground using a mortar and pestle. An accurately weighed portion of approximately 88.32 mg of the powdered sample was transferred to a 50.0 mL volumetric flask and dissolved in a 0.10 mol L^{-1} NaOH solution. The solution was placed in an ultrasonic bath for 20

minutes to ensure complete dissolution. In the final step, it was diluted to the required concentrations using a supporting electrolyte. The synthetic urine sample was prepared following the procedure described by Laube et al.[19] Specifically, 0.73 g of NaCl, 0.40 g of KCl, 0.28 g of $CaCl_2 \cdot 2H_2O$, 0.56 g of Na_2SO_4, 0.35 g of KH_2PO_4, 0.25 g of NH_4Cl, and 6.25 g of urea were dissolved in water in a 250.0 mL volumetric flask. This mixture was then diluted in a 0.10 mol L^{-1} NaOH solution at a 1:10 ratio and supplemented with three varying concentrations of NMS.

RESULTS AND DISCUSSION

Electrochemical behavior of NMS

The initial study focused on investigating the electrochemical behavior of NMS across a wide potential range, as this analyte contains two redox centers within its molecule: the $–NO_2$ group, which undergoes reduction at more negative potentials, and the –NH group, which oxidizes at less negative potentials. To ensure accurate measurements, oxygen was removed from the solution, as its presence could interfere at negative potentials. Figure S1 shows the cyclic voltammogram obtained over a potential range of +1.5 to -1.2 V. Two reduction peaks are observed at approximately 0.0 V and -0.5 V, corresponding to the reduction of the nitro group and its derivatives. These form two redox pairs with oxidation peaks around +0.06 V and +0.6 V. The oxidation peaks observed beyond these potentials are associated with the –NH group.[20-22]

This work focuses on developing a simple and rapid method for the determination of NMS. A potential range of +0.5 to +1.3 V was selected to avoid interference from oxygen reduction and the formation of byproducts at more negative potentials. As shown in Figure 1A, an anodic peak (Ipa) was observed at approximately +1.0 V, with no corresponding reduction peak, indicating that the electrode process in this potential window is irreversible. Similar behavior has been reported in previous studies on NMS oxidation,[1,13] and according to the literature, this anodic peak is attributed to the irreversible oxidation of the methylsulfonamide group in the NMS structure.[23,24] Although nimesulide exhibits multiple electrochemical processes, as evidenced in Figure S1, the analytical strategy adopted in this work was based on the selective use of this single redox process, which provides a well-defined, intense, and reproducible voltammetric signal within a safe potential window, thereby minimizing matrix interferences and electrode fouling. While the simultaneous exploration of multiple redox processes could, in principle, enhance selectivity, it generally increases methodological complexity and reduces robustness for routine analysis. Therefore, the selected anodic process represents the best compromise between sensitivity, selectivity, and operational simplicity for practical sensor applications.

The mass transport of the NMS molecule at the proposed electrode was investigated using a 0.12 mol L^{-1} PB solution containing 30.0 µmol L^{-1} NMS, with a scan rate range from 10 to 100 mV s^{-1} (see Figure 1B). The relationship between the peak current and the square root of the scan rate (Figure 1C) exhibited good linearity, with a correlation coefficient of 0.9978. This result suggests that the electron-transfer process governing mass transport occurs via diffusion. To validate this finding further, the relationship between the logarithm of the peak current and the logarithm of the scan rate (Figure 1D) was examined, leading to the equation $\text{Log } I_p = 0.426 \text{ Log } v – 0.514$. In such analyses, coefficients near 0.5 or 1.0 usually suggest that mass transfer is mainly governed by diffusion or adsorption, respectively.[25,26] The coefficient derived in this research suggests that the electron-transfer process controlling the mass transport of NMS at the proposed electrode is primarily diffusion-driven, consistent with existing literature.[27,28]

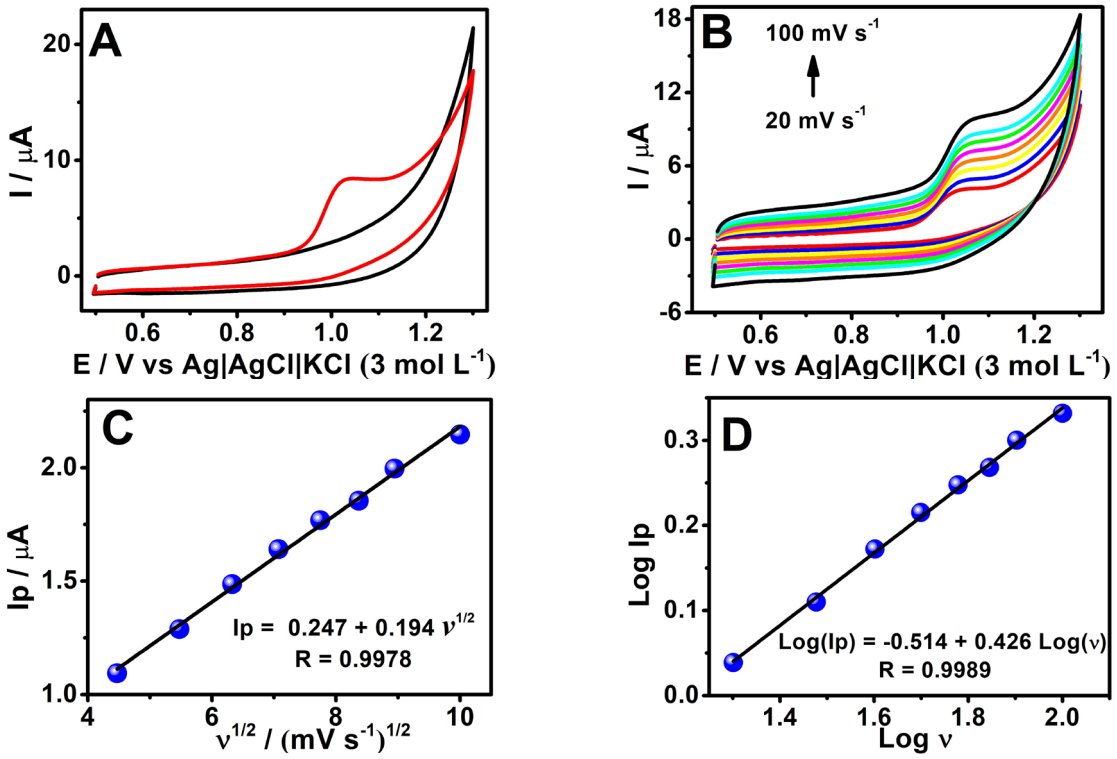

Figure 1. Cyclic voltammograms were obtained using LIGe in a 0.12 mol L^{-1} PB solution at pH 5.00. (A) The response is shown without (black line) and with (red line) 30.0 μmol L^{-1} NMS. The instrumental settings were a scan rate of 50 mV s^{-1} and a step potential of 5 mV s^{-1}. (B) Voltammograms at varying scan rates (v) from 10 to 100 mV s^{-1} in the presence of 30.0 μmol L^{-1} NMS. (C) The relationship between the peak current (Ip) and the square root of the scan rate ($v^{1/2}$). (D) The relationship between the logarithm of the peak current (log Ip) and the logarithm of the scan rate (log v).

The kinetic parameters of the electrode process were further investigated. Based on the Laviron theory for irreversible systems, the relationship between the peak potential (E_p) and the natural logarithm of the scan rate (ln(v)) was analyzed (Figure S2). From this analysis, the charge transfer coefficient (α) was determined to be 0.9, and the number of electrons (n) transferred in the process was calculated as 1.7. This value is close to 2, which is consistent with the NMS oxidation mechanism reported in the literature.[13,23,27,28]

Through the pH study (Figure 2), the Nernst equation was used to determine the proton-to-electron ratio involved in the oxidation of NMS on the LIGe surface.[29] The slope obtained was 63.4 mV/pH. This value is very close to the theoretical slope of 59.2 mV per pH unit at 25 °C for a 1:1 proton-to-electron ratio. These results suggest an oxidation mechanism involving the transfer of two protons and two electrons. Regarding the optimal pH for analysis, the maximum current was obtained at pH 2.00. However, this potential is undesirably high, as it increases the risk of interference from other electroactive species, potentially compromising selectivity. Consequently, pH 7.00 was selected for subsequent studies, as it provided a high current response at a more favorable potential.

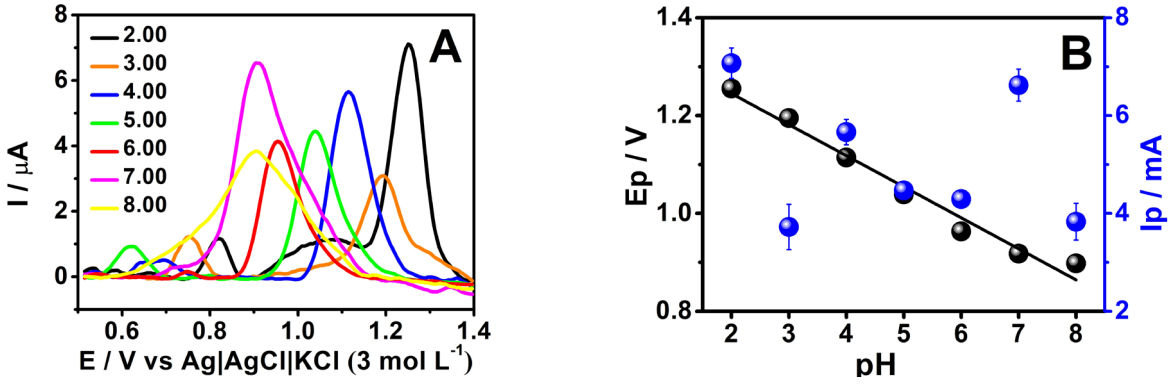

Figure 2. (A) Square wave voltammograms recorded with LIGe in the presence of NMS (10.0 µmol L^{-1}) in BR buffer solution (0.12 mol L^{-1}) at different pH values (2.00 – 8.00). (B) Dependence of the peak current (Ip) and peak potential (Ep) on the pH of the medium. Experimental conditions: amplitude = 60 mV; frequency = 10 Hz; potential increment = 5 mV.

SWV system optimization and analytical performance

To enhance the experimental conditions, the parameters of SWV, including pulse amplitude (20 to 100 mV), potential increment (2 to 10 mV), and frequency (5 a 25 Hz), were systematically optimized (Figure S3). These evaluations were conducted using a 10.0 µmol L^{-1} NMS solution prepared in 0.12 mol L^{-1} PB at pH 7.00. The selection of the optimal parameters was guided by criteria such as stability, reproducibility, current intensity, and peak resolution, ensuring robust and precise analytical performance. The optimal analytical parameters for NMS determination using SWV are summarized in Table I. Therefore, the optimal values of the SWV operational parameters chosen were frequency (*f*) = 15 Hz, amplitude (*a*) = 60 mV, and step potential (ΔE) = 10 mV.

Table I. Experimental parameters evaluated for SWV technique, and the corresponding values selected for determining NMS

Parameter	Range	Optimized
Frequency (Hz)	5 to 25	15
Amplitude (mV)	20 to 100	60
Step potential (mV)	2 to10	10

After optimizing the SWV parameters, the analytical curve was constructed by successively adding aliquots of the stock solution (1.0 mmol L^{-1}) of NMS into the electrochemical cell containing 0.12 mol L^{-1} PB (pH 7.00) using the LIGe. As shown in Figure 3, the analytical curve exhibited linearity in the concentration range of 11.0 to 131 µmol L^{-1}, following the linear regression equation: Ip (µA) = 5.00 + 0.181C_{NMS} (µmol L^{-1}), with r^2 = 0.999. The equations LOD = 3.3 s/b and LOQ = 10 s/b were employed to determine the limits of detection (LOD) and quantification (LOQ), where s represents the standard deviation of the blank and b denotes the slope of the analytical curve. The LOD and LOQ were found to be 1.30 and 4.30 µmol L^{-1}, respectively.

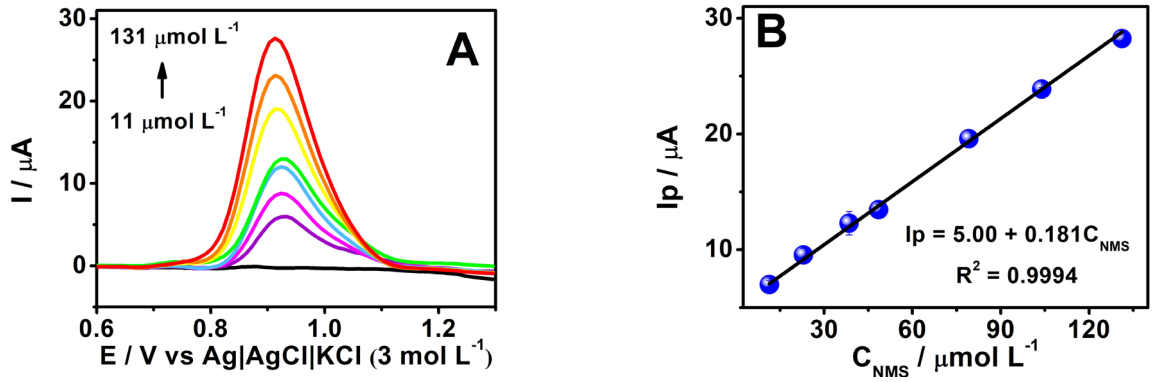

Figure 3. (A) Square wave voltammograms obtained using LIGe for NMS concentrations ranging from 11.0 to 131 μmol L^{-1} in 0.12 mol L^{-1} PB (pH 7.00). SWV parameters: *f* = 15 Hz, *a* = 60 mV, *ΔEs* = 10 mV. (B) Analytical curve (Ip *vs*. C_{NMS}).

The analytical performance of the proposed unmodified LIG sensor should be interpreted in the context of both its intended application and the fabrication strategy adopted. As summarized in Table II, electrochemical sensors for nimesulide span a broad spectrum of analytical characteristics. Methods based on nanocomposites or chemically modified electrodes typically achieve detection limits in the nanomolar range; however, they require complex multi-step fabrication procedures, including nanoparticle synthesis, polymer electrodeposition, or composite formulation, which substantially increase preparation time and experimental complexity.

In contrast, the unmodified LIG electrode developed in this work provides a wide linear range of 11–131 μmol L^{-1} (120 μmol L^{-1} span), which is comparable to or broader than that reported for many modified electrodes, despite the complete absence of chemical modification. Among unmodified electrodes reported in the literature, the present sensor exhibits one of the widest working ranges, while maintaining straightforward fabrication by direct CO_2 laser ablation.

Although the detection limit (1.30 μmol L^{-1}) is higher than those achieved by heavily modified sensors, this value is fully adequate for pharmaceutical quality control, where typical working concentrations after sample preparation are on the order of 50–200 μmol L^{-1}. In this application context, ultra-low detection limits are not a strict requirement, whereas a broad linear range, minimal sample dilution, and operational simplicity are highly advantageous. The results therefore demonstrate a deliberate trade-off between ultimate sensitivity and practical applicability, favoring simplicity, scalability, and reproducibility.

Table II. Comparison of analytical parameters obtained by different methods reported in the literature for NMS determination

Electrode	Technique	Linear Range (μmol L^{-1})	LOD (μmol L^{-1})	Samples	Ref.
BNC/CPE	SWV	0.01 – 0.55	11×10^{-3}	Urine / Pharmaceutical Samples	30
3D-printed CB/PLA	DPV	1 – 75	0.193	Wastewater	31
SiC-NPs/GCE	DPV	0.9 – 8.7	0,03	Human blood serum	32
GR/p(L-Cys)/GCE	DPV	1.0 – 55.0	0.3	Tap Water / River Water	28
LIGe	**SWV**	**11.0 – 131.0**	**1.29**	**Urine / Pharmaceutical Samples**	**This work**

BNC: bentonite clay; CPE: Carbon paste electrode; GR/p(L-Cys): poly(L-cysteine) and graphene composite; GCE: Glassy Carbon Electrode; SiC-NPs: Carbon silica nanoparticles; CB/PLA: carbon black/filled polylactic acid.

To assess the precision of the proposed method for the determination of NMS, a repeatability study was conducted based on the analytical signal obtained from 10 consecutive measurements in a standard solution of NMS (30.0 μmol L^{-1}) under optimized conditions. From the results presented in Figure S4, it can be observed that there was no significant variation in current values, as the relative standard deviation (RSD) of the analysis is below 5%. This indicates good stability in the electrode response and suggests that no significant decrease in electrode activity was observed.

An interference study was conducted using the SWV technique. The effect of potential interferents was evaluated at 1:10 ratio (NMS:interferents) by comparing the anodic peak currents obtained in absence and presence of each species (Table III). As observed, there was no significant interference in the determination of NMS, as the variations remained below 3.0%. Therefore, the methodology can be effectively applied for NMS detection even in the presence of these species.

Table III. Effect of potential interferents on the voltammetric determination of NMS at a concentration level of 1.0 mmol L^{-1}

Interferent	Interferent Ratio	Ip Variation (%)
Urea	1:10	2.24
Glicose	1:10	0.37
Oxalic Acid	1:10	2.66
Citric Acid	1:10	2.27

Sample analysis

To analyze the pharmaceutical sample, NMS determination was performed using the external calibration curve equation: $Ip(\mu A) = 5.00 + 0.181C_{NMS}$ (μmol L^{-1}). For the pharmaceutical samples, the result obtained was 101 mg/tablet of NMS. According to the information provided by the manufacturer, the declared NMS mass per tablet is 100 mg. This result aligns with the specifications presented in the pharmacopeia, which establishes a minimum of 95% and a maximum of 105% of the declared NMS content in tablets.[33] The determination of NMS was also carried out in synthetic urine samples at three different concentrations (44.4, 58.4, and 85.1 μmol L^{-1}), and the analysis was based on an external calibration curve (Figure S5), given by the equation $Ip(\mu A) = 5.28 + 0.196C_{NMS}$ (μmol L^{-1}), and the results were assessed in terms of percentage recovery, as summarized in Table IV.

It should be noted that the concentrations of nimesulide evaluated in synthetic urine were selected exclusively for analytical validation purposes and were not intended to reproduce physiological urinary levels. Under therapeutic conditions, nimesulide undergoes extensive hepatic metabolism, and less than 0.5% of the administered dose is excreted in urine as unchanged drug, with elimination occurring predominantly as hydroxylated and conjugated metabolites, especially 4′-hydroxynimesulide.[34,35] Radiolabeled studies further confirm that urinary excretion reflects metabolic products rather than the parent compound.[34,36] Therefore, the concentration levels employed in synthetic urine were chosen to fall within the linear working range of the sensor and to ensure reliable evaluation of accuracy and recovery in a complex matrix, rather than to simulate real urinary concentrations.

Table IV. Determination of NMS in synthetic urine samples

Sample	Spiked (μmol L^{-1})	Found (μmol L^{-1})	Recovery (%)
Synthetic urine	44.4	42.9 ± 1.5	97
	58.4	63.8 ± 5.4	109
	85.1	94.8 ± 9.7	111

CONCLUSION

This work demonstrates, for the first time, the potential of unmodified laser-induced graphene (LIG) electrodes for the electrochemical determination of nimesulide. Voltammetric studies showed that NMS oxidation is an irreversible, diffusion-controlled process involving the transfer of two protons and two electrons. Systematic optimization of experimental parameters (electrolyte pH and SWV conditions) resulted in reliable analytical performance, with a wide linear range of 11.0–131 μmol L^{-1} (120 μmol L^{-1} span) and a detection limit of 1.30 μmol L^{-1}. The sensor was successfully applied to pharmaceutical tablets, providing results consistent with the declared content (101 mg per tablet versus 100 mg per tablet). Recovery values in synthetic urine ranged from 97% to 111%, indicating acceptable accuracy in a complex matrix. Interference studies demonstrated that common non-electroactive urinary constituents, such as urea, glucose, oxalic acid, and citric acid, caused only minor signal variations (<3%), supporting adequate selectivity toward these species. Importantly, the main contribution of this work does not lie in achieving the lowest detection limit reported in the literature, but in combining a broad linear working range with extremely simplified fabrication, eliminating chemical modification and nanomaterial synthesis. Although the detection limit is higher than that of ultra-sensitive modified electrodes, it is fully adequate for pharmaceutical quality control applications, where analyte concentrations are typically much higher. The balance between analytical performance, fabrication speed, low cost, and disposability positions the proposed unmodified LIG sensor as a practical and attractive alternative for routine analysis and rapid screening, while further studies in real biological samples are encouraged to expand its clinical relevance. Further validation using multiple independent samples, statistical comparison tests, and reference analytical methods is required to fully establish the accuracy of the proposed sensor.

Acknowledgements

The authors are grateful for the financial support provided by the Brazilian agencies Fundação de Amparo à Pesquisa e ao Desenvolvimento Científico e Tecnológico do Maranhão – FAPEMA (00930/22, 00901/22); Coordenação de Aperfeiçoamento de Pessoal de Nível Superior – CAPES (Finance Code 001, 88887.658022/2021-00), and Conselho Nacional de Desenvolvimento Científico e Tecnológico – CNPq (444777/2024-5).

Conflicts of interest

The authors declare no competing financial interest.

Use of Artificial Intelligence (AI) tools

The authors acknowledge using the Grammarly tool exclusively for linguistic revision to improve clarity, grammar, spelling, and fluency. The AI tool Google Gemini was used to generate part of the graphical abstract. The authors take full responsibility for the accuracy, integrity, and originality of the work and confirm that no AI tools were used to generate scientific ideas, analyze data independently, or replace the authors' critical role.

REFERENCES

(1) de Oliveira, W. B. V.; Lisboa, T. P.; de Souza, C. C.; Matos, M. A. C.; Matos, R. C. Composite Material Immobilized in 3D-Printed Support, an Economical Approach for Electrochemical Sensing of Nimesulide. *Microchem. J.* **2023**, *188*, 108463. https://doi.org/10.1016/j.microc.2023.108463

(2) Ho, C. V.; Pazourek, J. Rapid Determination of Nimesulide by Capillary Zone Electrophoresis in Various Pharmaceutical Formulations. *Separations* **2025**, *12* (5), 132. https://doi.org/10.3390/separations12050132

(3) de Almeida, A. C.; Ferreira, P. O.; Porto, M. V.; Canotilho, J.; de Castro, R. A. E.; Caires, F. J.; Eusébio, M. E. S. Novel Nimesulide Multicomponent Solid Forms: Screening, Synthesis, Thermoanalytical Study and Characterization. *J. Therm. Anal. Calorim.* **2025**, *150*, 6885-6897. https://doi.org/10.1007/s10973-024-13189-2

(4) Regi, J. K.; Lalwani, K.; Pawar, S. Comparative Trends in the Usage of Nonsteroidal Anti-Inflammatory Drugs: Self-Administration versus Prescription. *MGM Journal of Medical Sciences* **2024**, *11* (1), 139–145. https://doi.org/10.4103/mgmj.mgmj_145_22
(5) Arfeen, M.; Srivastava, A.; Srivastava, N.; Khan, R. A.; Almahmoud, S. A.; Mohammed, H. A. Design, Classification, and Adverse Effects of NSAIDs: A Review on Recent Advancements. *Bioorg. Med. Chem.* **2024**, *112*, 117899. https://doi.org/10.1016/j.bmc.2024.117899
(6) Yue, X.; Xu, X.; Liu, C.; Zhao, S. Simultaneous Determination of Cefotaxime and Nimesulide Using Poly(L-Cysteine) and Graphene Composite Modified Glassy Carbon Electrode. *Microchem. J.* **2022**, *174*, 107058. https://doi.org/10.1016/j.microc.2021.107058
(7) Lavande, J. P.; Bais, S. K.; Kharat, V. Active Pharmaceutical Ingredient and Impurity Profiling Nimesulide. *International Journal of Advanced Research in Science, Communication and Technology* **2023**, 525–536. https://doi.org/10.48175/IJARSCT-9248
(8) Pandey, S. K.; Pudasaini, J.; Parajuli, H.; Singh, R. E.; Shah, K. P.; Adhikari, A.; Rokaya, R. K. Formulation and Evaluation of Floating Tablet of Nimesulide by Direct Compression Method. *Magna Scientia Advanced Research and Reviews* **2024**, *10* (1), 153–161. https://doi.org/10.30574/msarr.2024.10.1.0008
(9) Kamble, S.; Bangale, G.; Deshmukh, R.; Dawargave, K.; Shingare, D.; Suryawanshi, O.; Kadam, K. Development and Optimization of Nimesulide Loaded Transethosomal Gel. *Bionanoscience* **2025**, *15* (2), 223. https://doi.org/10.1007/s12668-025-01802-z
(10) Waheb, A. A.; Rasheed, A. S.; Hassan, M. J. M. Strategies for the Separation and Quantification of Non-Steroidal Anti- Inflammatory Drugs Using ZIC-HILIC-HPLC with UV Detection. *Curr. Pharm. Anal.* **2022**, *18* (10), 949–958. https://doi.org/10.2174/1573412918666220915090831
(11) Sheikholeslami, M. N.; Gómez-Canela, C.; Barron, L. P.; Barata, C.; Vosough, M.; Tauler, R. Untargeted Metabolomics Changes on Gammarus Pulex Induced by Propranolol, Triclosan, and Nimesulide Pharmaceutical Drugs. *Chemosphere* **2020**, *260*, 127479. https://doi.org/10.1016/j.chemosphere.2020.127479
(12) Łysoń, M.; Górska, A.; Paczosa-Bator, B.; Piech, R. Nimesulide Determination on Carbon Black-Nafion Modified Glassy Carbon Electrode by Means of Adsorptive Stripping Voltammetry. *Electrocatalysis* **2021**, *12* (6), 641–649. https://doi.org/10.1007/s12678-021-00676-5
(13) Deroco, P. B.; Rocha-Filho, R. C.; Fatibello-Filho, O. A New and Simple Method for the Simultaneous Determination of Amoxicillin and Nimesulide Using Carbon Black within a Dihexadecylphosphate Film as Electrochemical Sensor. *Talanta* **2018**, *179*, 115–123. https://doi.org/10.1016/j.talanta.2017.10.048
(14) Inlumphan, S.; Wongwiriyapan, W.; Khemasiri, N.; Rattanawarinchai, P.; Leepheng, P.; Luengrojanakul, P.; Wuttikhun, T.; Obata, M.; Fujishige, M.; Takeuchi, K.; et al. Laser-Induced Graphene Electrochemical Immunosensors for Rapid and Sensitive Serological Detection: A Case Study on Dengue Detection Platform. *Sensors and Actuators Reports* **2025**, *9*, 100276. https://doi.org/10.1016/j.snr.2024.100276
(15) Matias, T. A.; Rocha, R. G.; Faria, L. V.; Richter, E. M.; Munoz, R. A. A. Infrared Laser-Induced Graphene Sensor for Tyrosine Detection. *ChemElectroChem* **2022**, *9* (14). https://doi.org/10.1002/celc.202200339
(16) Matias, T. A.; de Faria, L. V.; Rocha, R. G.; Silva, M. N. T.; Nossol, E.; Richter, E. M.; Muñoz, R. A. A. Prussian Blue-Modified Laser-Induced Graphene Platforms for Detection of Hydrogen Peroxide. *Microchim. Acta* **2022**, *189* (5), 188. https://doi.org/10.1007/s00604-022-05295-5
(17) Ferreira, D. C. M.; Inoque, N. I. G.; Tanaka, A. A.; Dantas, L. M. F.; Muñoz, R. A. A.; da Silva, I. S. Lab-Made CO_2 Laser-Engraved Electrochemical Sensors for Ivermectin Determination. *Anal. Methods* **2024**, *16* (25), 4136–4142. https://doi.org/10.1039/D4AY00414K
(18) Wanjari, V. P.; Kumar, P.; Duttagupta, S. P.; Singh, S. P. Adsorption-Enhanced Sensitivity for Electrochemical Sensing of Diclofenac by Poly(Ether Sulfone)-Based Laser-Induced Graphene. *Langmuir* **2025**, *41* (1), 152–161. https://doi.org/10.1021/acs.langmuir.4c03229

(19) Laube, N.; Mohr, B.; Hesse, A. Laser-Probe-Based Investigation of the Evolution of Particle Size Distributions of Calcium Oxalate Particles Formed in Artificial Urines. *J. Cryst. Growth* **2001**, *233* (1–2), 367–374. https://doi.org/10.1016/S0022-0248(01)01547-0
(20) Moscoso, R.; Álvarez-Lueje, A.; Squella, J. A. Nanostructured Interfaces Containing MWCNT and Nitro Aromatics: A New Tool to Determine Nimesulide. *Microchem. J.* **2020**, *159*, 105361. https://doi.org/10.1016/j.microc.2020.105361
(21) Goularte, R. B.; Winiarski, J. P.; Latocheski, E.; Jost, C. L. Novel Analytical Sensing Strategy Using a Palladium Nanomaterial-Based Electrode for Nimesulide Electrochemical Reduction. *J. Electroanal. Chem.* **2022**, *920*, 116622. https://doi.org/10.1016/j.jelechem.2022.116622
(22) Miranda, L.; Pereira, V. C.; Machado, C. S.; Torres, Y. R.; dos Anjos, V. E.; Quináia, S. P. Direct Determination of Nimesulide in Natural Waters and Wastewater by Cathodic Stripping Voltammetry. *Arch. Environ. Contam. Toxicol.* **2017**, *73* (4), 631–640. https://doi.org/10.1007/s00244-017-0425-6
(23) Bukkitgar, S. D.; Shetti, N. P.; Kulkarni, R. M.; Halbhavi, S. B.; Wasim, M.; Mylar, M.; Durgi, P. S.; Chirmure, S. S. Electrochemical Oxidation of Nimesulide in Aqueous Acid Solutions Based on TiO2 Nanostructure Modified Electrode as a Sensor. *J. Electroanal. Chem.* **2016**, *778*, 103–109. https://doi.org/10.1016/j.jelechem.2016.08.024
(24) da Silva, I. S.; Capovilla, B.; Freitas, K. H. G.; Angnes, L. Strategies to Avoid Electrode Fouling for Nimesulide Detection Using Unmodified Electrodes. *Anal. Methods* **2013**, *5* (14), 3546. https://doi.org/10.1039/c3ay40463c
(25) Fatibello-Filho, O.; Silva, T.; Moraes, F.; Sitta, E. *Eletroanálises - Aspectos Teóricos e Práticos.* EDUFSCAR, Ed., São Carlos, SP, 2022.
(26) Pacheco, W. F.; Semaan, F. S.; Almeida, V. G. K.; Ritta, A. G. S. L.; Aucélio, R. Q. Voltammetry: A Brief Review About Concepts. *Rev. Virtual Quim.* **2013**, *5* (4). https://doi.org/10.5935/1984-6835.20130040
(27) Shetti, N. P.; Malode, S. J.; Nayak, D. S.; Bukkitgar, S. D.; Bagihalli, G. B.; Kulkarni, R. M.; Reddy, K. R. Novel Nanoclay-Based Electrochemical Sensor for Highly Efficient Electrochemical Sensing Nimesulide. *J. Phys. Chem. Solids* **2020**, *137*, 109210. https://doi.org/10.1016/j.jpcs.2019.109210
(28) Yue, X.; Xu, X.; Liu, C.; Zhao, S. Simultaneous Determination of Cefotaxime and Nimesulide Using Poly(L-Cysteine) and Graphene Composite Modified Glassy Carbon Electrode. *Microchem. J.* **2022**, *174*, 107058. https://doi.org/10.1016/j.microc.2021.107058
(29) Dai, C.; Crawford, L. P.; Song, P.; Fisher, A. C.; Lawrence, N. S. A Novel Sensor Based on Electropolymerized Substituted-Phenols for PH Detection in Unbuffered Systems. *RSC Adv.* **2015**, *5* (126), 104048–104053. https://doi.org/10.1039/C5RA22595G
(30) Prabhu, K.; Malode, S. J.; Veerapur, R. S.; Shetti, N. P. Clay-Based Carbon Sensor for Electro-Oxidation of Nimesulide. *Mater. Chem. Phys.* **2021**, *272*, 124992. https://doi.org/10.1016/j.matchemphys.2021.124992
(31) Cieślik, M.; Rucka, M.; Siqueira, G. P.; Koterwa, A.; Rycewicz, M.; Muñoz, R. A. A.; Bogdanowicz, R.; Ryl, J. Multi-Material Integrated 3D-Printed Electrochemical Detection Platform for Rapid on-Site Screening of Nimesulide in Industrial Sewage. *Microchim. Acta* **2025**, *192* (11), 757. https://doi.org/10.1007/s00604-025-07634-8
(32) Ghavami, R.; Navaee, A. Determination of Nimesulide in Human Serum Using a Glassy Carbon Electrode Modified with SiC Nanoparticles. *Microchim. Acta* **2012**, *176* (3–4), 493–499. https://doi.org/10.1007/s00604-011-0710-4
(33) *Farmacopeia Brasileira* (5th Ed.) 2010, *1*, 1–523.
(34) Bernareggi, A. Clinical Pharmacokinetics of Nimesulide. *Clin. Pharmacokinet.* **1998**, *35* (4), 247–274. https://doi.org/10.2165/00003088-199835040-00001
(35) Carini, M.; Aldini, G.; Stefani, R.; Marinello, C.; Facino, R. M. Mass Spectrometric Characterization and HPLC Determination of the Main Urinary Metabolites of Nimesulide in Man. *J. Pharm. Biomed. Anal.* **1998**, *18* (1–2), 201–211. https://doi.org/10.1016/S0731-7085(98)00172-1

(36) Macpherson, D.; Best, S. A.; Gedik, L.; Hewson, A. T.; Rainsford, K. D.; Parisi, S. The biotransformation and pharmacokinetics of 14C-nimesulide in humans following a single dose oral administration. *J. Drug. Metab. Toxicol.* **2012**, *4* (01). https://doi.org/10.4172/2157-7609.1000140

SUPPLEMENTARY MATERIAL

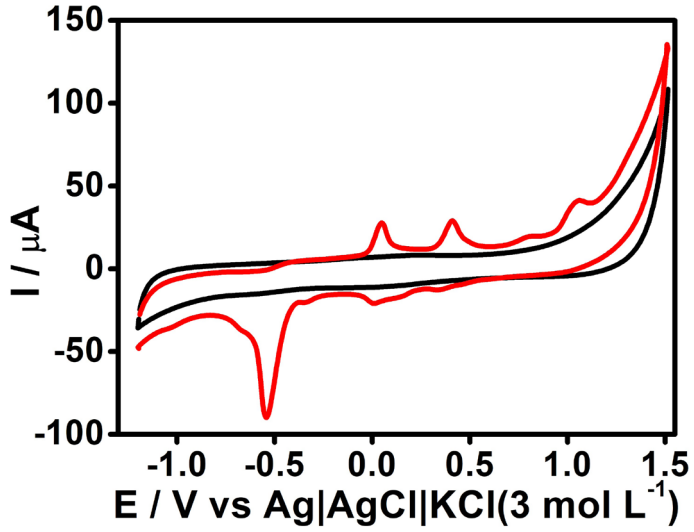

Figure S1. Cyclic voltammograms recorded in 0.12 mol L^{-1} PB solution pH 5.00 in the absence (black line) and presence (red line) of 100 µmol L^{-1} NMS. Instrumental conditions: scan rate = 50 mV s^{-1} and step potential = 5 mV s^{-1}.

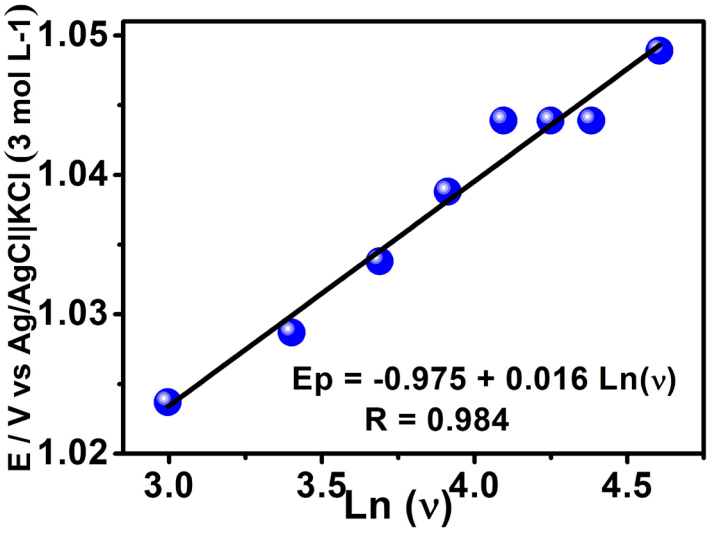

Figure S2. Dependence of the peak potential (Ep) on the natural logarithm of v in the presence of 30.0 µmol L^{-1} NMS. Experimental conditions: PB 0.12 mol L^{-1}; pH 5.00.

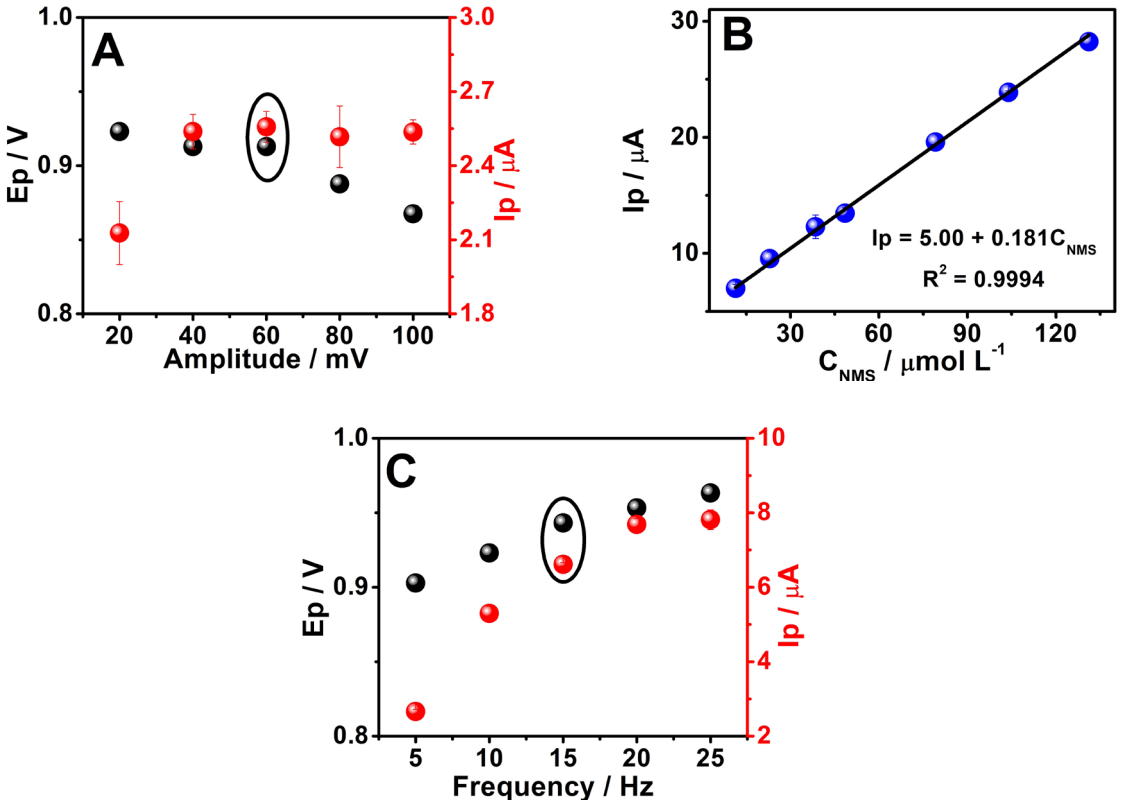

Figure S3. Optimizations of the SWV parameters: (A) amplitude (20.0 to 100 mV), (B) step potential (2.0 to 10.0 mV), and (C) frequency (5.0 to 25.0 Hz), in the presence of 10 μmol L^{-1} NMS. Experimental conditions: PB 0.12 mol L^{-1}; pH 7.00.

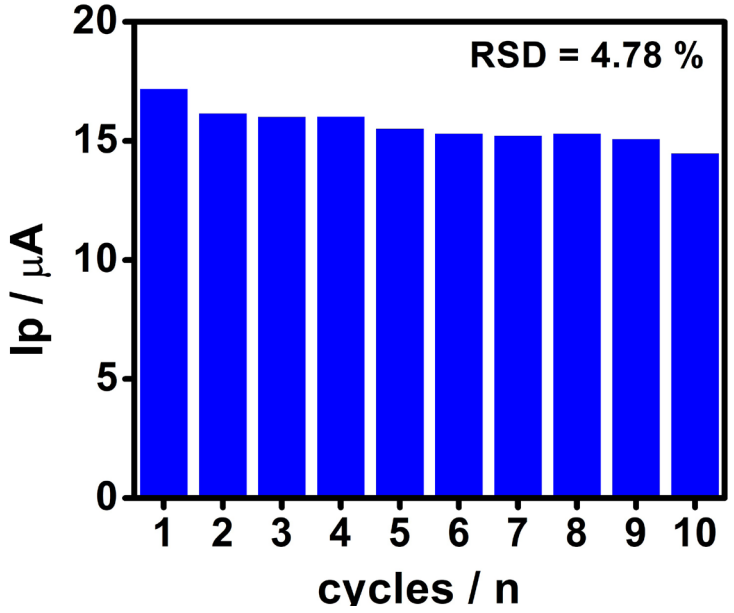

Figure S4. Repeatability study (*n*=10) of the LIGe electrode in the presence of NMS (30 μmol L^{-1}). Experimental conditions: 0.12 mol L^{-1} phosphate buffer; pH 7.0; a = 60 mV; f = 15 Hz; ΔEs = 10mV.

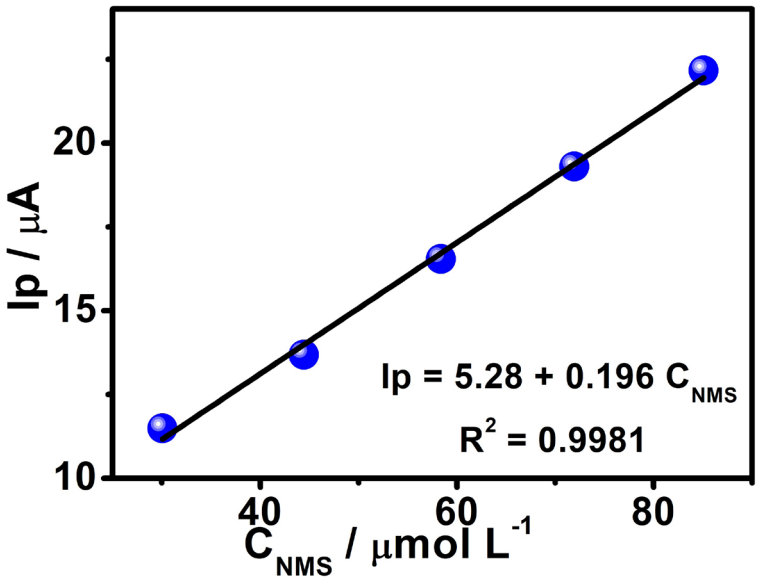

Figure S5. (A) Square wave voltammograms obtained using LIGe for NMS concentrations (44.4, 58.4, and 85.1 μmol L^{-1}) in synthetic urine. (B) External calibration curve (Ip vs. C_{NMS}). SWV parameters: *f* = 15 Hz, *a* = 60 mV, *ΔEs* = 10mV